OIKOS

Research

A macro-ecological approach to predation density-dependence

Matthieu Barbier, Laurie Wojcik and Michel Loreau

M. Barbier (https://orcid.org/0000-0002-0669-8927) ✉ (contact@mrcbarbier.org), L. Wojcik and M. Loreau, Centre for Biodiversity Theory and Modelling, Theoretical and Experimental Ecology Station, UMR 5321, CNRS and Paul Sabatier Univ., Moulis, France.

Oikos
130: 553–570, 2021
doi: 10.1111/oik.08043

Subject Editor and
Editor-in-Chief: Dries Bonte
Accepted 3 January 2021

Predation often deviates from the law of mass action: many micro- and meso-scale experiments have shown that consumption saturates with resource abundance, and decreases due to interference between consumers. But does this observation hold at macro-ecological scales, spanning many species and orders of magnitude in biomass? If so, what are its consequences for large-scale ecological patterns and dynamics?

We perform a meta-analysis of predator–prey pairs of mammals, birds and reptiles, and show that total predation rates appear to increase, not as the product of predator and prey densities following the Lotka–Volterra (mass action) model, but rather as the square root of that product. This suggests a phenomenological power-law expression of the effective cross-ecosystem predation rate. We discuss whether the same power-law may hold dynamically within an ecosystem, and assuming that it does, we explore its consequences in a simple food chain model. The empirical exponents fall close to the boundary between regimes of donor and consumer limitation. Exponents on this boundary are singular in multiple ways. First, they maximize predator abundance and some stability metrics. Second, they create proportionality relations between biomass and productivity, both within and between trophic levels. These intuitive relations do not hold in general in mass action models, yet they are widely observed empirically.

These results provide evidence of mechanisms limiting predation across multiple ecological scales. Some of this evidence was previously associated with donor control, but we show that it supports a wider range of possibilities, including forms of consumer control. As limiting consumption counter-intuitively allows larger populations, it is worthwhile to reconsider whether the observed predation rates arise from microscopic mechanisms, or could hint at selective pressure at the population level.

Keywords: functional response, macroecology, predation, scaling laws, trophic ecology

Introduction

Many dynamical food web models attempt to represent population-level dynamics by zooming out from the microscopic complexity of individual predator and prey behavior, physiology and ecology. Since Lindeman (1942), these models have shared the same fundamental structure, i.e. a balance of energy gains and losses from predation and from non-trophic processes. The hidden complexity and specificity of a given ecosystem is generally summarized in a simple function which describes how predation

NORDIC SOCIETY OIKOS

www.oikosjournal.org

and energy fluxes between trophic levels depend on stocks at each level (predator and prey abundances). The most basic assumption is mass action: encounter probability increases as the product of predator and prey density. But natural settings often deviate from this baseline (Holling 1965). The expression of this function has been the topic of extensive empirical and theoretical inquiries, and even major debates (Arditi and Ginzburg 1989, Abrams 2015).

When we aim at large-scale prediction, the functional form in our equations does not represent the concrete mechanisms of predation – instead, its purpose is to express the cumulative effect of many predation events, aggregated over time and space, on the dynamics of large populations. For instance, we may hope to predict whether an entire regional population will show a strong response to invasions or exploitation, such as a trophic cascade or collapse (Pauly et al. 2000). Yet, modelling studies often simply resort to functional forms observed at a microscopic scale, such as the saturating functional response of a single predator. But there is no reason to expect that a single mathematical expression, whether mechanistic or phenomenological, will be appropriate to model all ecological processes (Aljetlawi et al. 2004, Barraquand 2014). We may have to derive different expressions for different questions and scales, from short-term laboratory experiments (Vucic-Pestic et al. 2010), through multi-generation predator–prey cycles (Turchin 2003), to macro-scale food web properties such as biomass pyramids and stability (Barbier and Loreau 2019).

Here we propose a new, empirically-motivated and phenomenological formulation for predation rates at large spatio–temporal scales. At these scales, the classic predator-oriented notion of functional response (Holling 1965) (how often a single predator will feed, depending on prey density) must be replaced by a more symmetrical notion: the total predation rate, or flux of biomass between predator and prey species, and how it is controlled by the two species' densities. This formulation acknowledges both predator and prey densities as potentially limiting, through a variety of mechanisms such as consumer interference, prey saturation, refuges, spatial structure, etc. By contrast with mechanistic theories (DeLong and Vasseur 2012, Pawar et al. 2012, DeLong et al. 2015, Portalier et al. 2019), our aim is not to ascertain the most realistic expression of predation rates, but to find a simple expression that can mimick observed rates across multiple scales, and then to understand its consequences for other food chain properties.

We first perform a meta-analysis of predation rates observed for higher vertebrates in the field, covering a range of species, study durations and areas. In the existing literature, most measurements of the predation rate as a function of predator and prey density come from feeding experiments, restricted to time scales far shorter than the predator's generation time (Skalski and Gilliam 2001, Pawar et al. 2012). While these experimental measurements are valuable for mechanistic models of specific populations, they may be misleading when extrapolating to macro-scale dynamics (Aljetlawi et al. 2004). For the latter, we need a phenomenological expression that exhibits some form of scale invariance, so that it may hold across different levels of aggregation. We propose a power-law expression similar to the Cobb–Douglas production function in economics (Cobb and Douglas 1928). We then find best-fit exponents suggesting a square root dependence of predation on both predator and prey density. These exponents are starkly lower than those expected from the simple mass action (Lotka–Volterra) model, suggesting that hidden mechanisms strongly limit predation.

This empirical trend can only be interpreted as a meaningful mathematical expression if it can be used to predict large-scale dynamics. This raises multiple questions. Knowing that local populations undergo many complex processes on short time scales, is it possible to write an effective model that approximates the dynamics of abundances aggregated over years and over whole landscapes? What kind of equations and nonlinearities should be used in this effective model? These questions have been raised in prior studies, mainly within the theoretical literature (Law and Dieckmann 1999, Pascual and Levin 1999, Barraquand and Murrell 2013, Hatton et al. 2015), which have shown that effective models can indeed be constructed in some cases, and may be quite different from the dynamics known at small scales. Being phenomenological, such models often cannot easily be interpreted in terms of concrete mechanisms or instantaneous demographic events. They generally do not exhibit the intuitive properties of classical functional responses (Morozov and Petrovskii 2013). But when successful, they can provide useful predictions. The present study should be viewed as exploratory, investigating one hypothetical way of describing large-scale, long-term dynamics by a simple set of effective differential equations.

An important question remains: how can we parameterize our effective model from observational data, collected within or across ecosystems? Indeed, the empirical relations between predation rates and densities of predators and prey do not necessarily translate directly to a true dynamical dependence between these three quantities. Other latent factors could be varying between measurements, and creating spurious relations. Nevertheless, we find hints that such confounding variation is weaker than the dependence that we wish to capture. We therefore assume that the observed scaling law can be inserted directly into a simple dynamical model, in order to explore its potential ecological consequences.

The empirical scaling exponents occupy a special position in our model, as they correspond to a maximum in predator abundance and some metrics of stability. While our sublinear model suggests that predation frequency is much lower than in a classic Lotka–Volterra model, it also leads to larger standing predator populations. This apparent paradox is closely related to the 'hydra effect', a term that originally applies to situations where increasing individual predator mortality leads to larger predator populations (Abrams 2009, Schröder et al. 2014), but can be extended to any situation, such as ours, where consumers that seem individually less fit (e.g. consume less prey than their competitors) may become more abundant in the long term (Abrams 2019).

A second unexpected consequence is the emergence of consistent scaling relationships between predator and prey densities, and between production and biomass within each trophic level. Such scaling laws are widely found in data and postulated in ecosystem models (Loreau 2010, Hatton et al. 2015). They are notably used in contexts of ecosystem management, such as fisheries (Borgmann 1987, Christensen and Walters 2004). But these relationships do not emerge spontaneously from arbitrary dynamical models, and only prevail under particular ecological conditions (Barbier and Loreau 2019). Our fitted exponents recover simple proportionality rules that are usually associated with donor control.

Our work raises the possibility that consumptive saturation and interference may happen at all scales, not only the classic scale of individual predator behavior (Holling 1965), and that this prevalence is tied to the empirical robustness of various allometric relationships, and the maximization of predator abundance and persistence.

Material and methods

Dataset

We compiled data from 32 observational studies (details in the Supporting information) that reported kill rates k_{12} (number of prey killed per predator per year) in the field, as well as prey density N_1 and predator density N_2. For each species, we also collected typical body mass measurements w (in kg) and mass-specific metabolic rate measurements m (in W kg^{-1}) from the AnAge database (De Magalhaes and Costa 2009) and two studies by White and Seymour (2003) and Makarieva et al. (2008), as these traits were rarely reported for the populations studied in the field (Brose et al. 2019). Whenever multiple values were found, we used the average values for each species.

The final dataset comprises 46 predator–prey pairs including 26 predator species and 32 prey species. Predator species belong to classes Mammalia, Aves and Reptilia, while prey species belong to classes Mammalia, Actinopterygii, Aves and Malacostraca.

For each predator–prey pair, we computed the rate of biomass loss in the prey population due to predation (in kg km^{-2} year^{-1}) as

$$C = k_{12} w_1 N_2 \tag{1}$$

and population biomass densities $B_1 = w_1 N_1$ and $B_2 = w_2 N_2$ in kg km^{-2}.

Food chain model

We investigate a simple food chain model of arbitrary length, where we follow the biomass density B_i of trophic level i as it changes through time,

$$\frac{dB_i(t)}{dt} = -\underbrace{L_i(t)}_{\text{internal losses}} + \underbrace{P_i(t)}_{\text{production}} - \underbrace{C_i(t)}_{\text{predation losses}} \tag{2}$$

where L_i and P_i represent internal losses and biomass production at level i, while C_i represents losses from predation by level $i+1$. Production at level 1 arises from autotrophic growth

$$P_1(t) = g_1 B_1(t) \tag{3}$$

while at higher levels, we assume

$$P_{i+1}(t) = \varepsilon C_i(t) \tag{4}$$

where ε (taken here to be constant for simplicity (The conversion rate ε is known to vary, but its range is limited compared to other quantities which can span orders of magnitude (Barbier and Loreau 2019). We choose to ignore ecological contexts in which predator production may be density-dependent even for a fixed amount of consumption, e.g. a reduced offspring number in denser groups, which could be represented by a function $\varepsilon(B_{i+1})$.)) is the conversion rate between the biomass lost through predation at level i and produced at level $i+1$. Internal losses can arise from individual metabolic costs and mortality, μ_i, and from self-regulation or density-dependent processes such as competition and pathogens, D_i,

$$L_i(t) = \mu_i B_i(t) + D_i B_i^2(t) \tag{5}$$

Alternatively, we later consider the possibility of a power-law expression $L_i(t) = D_i B_i^{\delta}(t)$ which can interpolate between these two types of losses.

In the following, we only consider stationary properties of the dynamics (Eq. 2), and thus drop the time-dependence of all quantities, which are assumed to take their equilibrium values.

Density-dependence

Throughout this study, we consider phenomenological mathematical expressions, emerging at the landscape level from unknown, potentially complex, underlying spatio–temporal dynamics (Barraquand and Murrell 2013). Consequently, these functions may not follow traditional expectations and intuitions derived from mechanistic functional responses (Morozov and Petrovskii 2013) – for instance, they might not scale additively with the number of prey or predator individuals or species.

While our data is always measured over large spatial scales compared to individual organism sizes, it still covers multiple orders of magnitude in spatial extension and biomass density. This can inform our choice of mathematical expression for the predation rate. Indeed, when considering phenomena that range over multiple scales, there are two common

possibilities: either there is a scale beyond which the phenomenon vanishes (for instance prey-dependence simply saturates past a critical density), or the phenomenon remains important at all scales. The second possibility drives us to search for a 'scale-free' mathematical expression, such as a power-law, which does not truly saturate but exhibits significant variation at all possible scales (Barenblatt 1996).

Following this argument, we choose here to focus on a 'scale-free' power-law dependence of predation losses (discussion in Box 1)

$$C_i \equiv C(B_i, B_{i+1}) = AB_i^{\beta} B_{i+1}^{\gamma} \tag{6}$$

with $\beta,\gamma \in [0,1]$, and A a constant which contains the attack rate, i.e. the basic frequency of encounters for a pair of predator and prey individuals. This attack rate may in principle be specific to each pair of species, while we assume that exponents β and γ are system-independent.

In this expression, $\beta=\gamma=1$ recovers the classic mass action (Lotka–Volterra) model. An exponent $\beta < 1$ is our counterpart to the well-studied phenomenon of prey saturation: predation does not truly saturate here (as the expression is scale-free), but it increases sublinearly with prey density, meaning that the ability of predators to catch or use each prey decreases with their availability (Holling 1965). On the other hand, $\gamma < 1$ indicates predator interference: larger predator densities lead to less consumption per capita (Skalski and Gilliam 2001). In the following, we will consider various arguments suggesting that empirical exponents may instead approximately satisfy the relationship $\beta+\gamma \approx 1$, which would imply a simpler ratio-dependent form

Box 1. Dimensional analysis

The difficulty of building a phenomenological cross-scale expression for predation rate is that it should account for both:

- between-systems parameter differences (e.g. different study areas, spatial structures, species traits),
- the within-system range of dynamical variables B_i that can lead to saturation and interference if they cross system-dependent thresholds.

We first appeal to dimensional analysis (Legendre and Legendre 2012). From Eq. 1 we see that predation losses C_i have the dimensions of biomass density over time, e.g. kg km^{-2} year^{-1}. A classic nondimensionalization choice (Yodzis and Innes 1992) is to express these losses using predator density and mass-specific metabolic rate (below for other options)

$$f_i = \frac{C_i}{m_{i+1}B_{i+1}} \tag{20}$$

where f_i is the normalized functional response (consumption per predator), incorporating all biological mechanisms. Since f_i has no dimension, it can only depend on dimensionless quantities. If we assume that all variation in predation is determined solely by species densities and metabolic rates, we can only construct two dimensionless ratios π_1 and π_2 and f_i must take the form

$$f_i = f\left(\pi_1 = \frac{m_i}{m_{i+1}}, \pi_2 = \frac{B_i}{B_{i+1}}\right) \tag{21}$$

with some arbitrary function f. The choice $f(\pi_1,\pi_2)=1$ leads to consumer dependence ($C_i=m_{i+1}B_{i+1}$), while $f(\pi_1,\pi_2)=\pi_1,\pi_2$ leads to donor dependence ($C_i=m_iB_i$). More generally, the Eq. 21 is strongly reminiscent of ratio-dependent functional response (Arditi and Ginzburg 2012), but it does not posit a specific functional form.

To deviate from this ratio-dependent expression, we must use additional parameters to construct other dimensionless quantities. Setting aside metabolic scaling for now, the Eq. 6 and 8 in the main text involve B_i and B_{i+1} separately, suggesting the form

$$f_i = f\left(\frac{B_i}{B_{i,\min}}, \frac{B_{i+1}}{B_{i+1,\min}}\right) \tag{22}$$

Indeed, it is plausible for nonlinear density-dependence in f to involve system-specific thresholds $B_{i,\min}$ (discussion in the Supporting information). These thresholds can be derived from other parameters that characterize each system, such as movement range or body mass. A further possibility, not investigated here, is that other biological rates may also intervene if metabolic rate cannot be used as a universal 'clock' for trophic processes (Glazier 2015).

Dimensionless ratios can capture important differences between systems, and a number of heuristics and mathematical theories exist to guide their choice (Barenblatt 1996): for instance, it is often useful to find ratios that are significantly larger than 1 in some systems and smaller than 1 in others, as this can indicate qualitatively different regimes. Thresholds such as $B_{i,\min}$ are commonly found in saturating functional responses (Holling 1965), where the density-dependence vanishes above a certain scale. If instead we expect a density-dependence that persists over a wide range of scales, we can use a 'scale-free' expression for the function f, such as a power-law (Barenblatt 1996).

$$C(B_i, B_{i+1}) \sim B_i^{\beta} B_{i+1}^{1-\beta} = B_{i+1} \left(\frac{B_i}{B_{i+1}} \right)^{\beta} \quad (7)$$

This relationship requires a strong effect of either or both interference and saturation.

These two predation-limiting phenomena are commonly reported and have been studied with various mathematical models. But classic functional responses generally go against our expectation of a 'scale-free' expression: they often assume that some density-dependence vanishes when density exceeds a particular scale or threshold. This may be realistic when depicting a given small-scale experimental system, but it is not adequate for data such as ours, compiled from different systems and scales. For instance, we can consider the standard saturating (Michaelis–Menten or Holling type 2) response (Holling 1965) and its extension, the DeAngelis–Beddington model (Beddington 1975, DeAngelis et al. 1975) with both saturation H and interference I

$$C(B_i, B_{i+1}) = \frac{AB_iB_{i+1}}{1 + HB_i + IB_{i+1}} \quad (8)$$

where H/A is traditionally defined as the handling time. This expression is applicable to short-term feeding experiments, where consumption is observed for a particular predator–prey species pair whose densities are imposed. The parameters H and I are contextual: they are expected to depend on species traits (Pawar et al. 2012), but also on the spatial structure and area of each study site. We discuss in Results and the Supporting information the difficulties associated with using this expression in a cross-ecosystem context.

Links between statistical and dynamical laws

We seek to identify the dynamical relationship $C(B_1,B_2)$ between predation losses and the biomasses of predator and prey in empirical data. In our theoretical analysis, we also discuss model predictions for another important observation, the scaling relations between production P and biomass B within and between trophic levels (Hatton et al. 2015).

Yet, the problem of relating cross-ecosystem statistical laws to underlying dynamical models is subtle, due to the potential covariance between variables and parameters. As a simple example, consider the scaling between production and biomass in one trophic level, assuming that the underlying dynamical law is $P(B) = rB$ with r a fixed growth rate. When we consider many ecosystems at equilibrium, each with a different growth rate, their values of r and B will likely be correlated. If they covary perfectly, the apparent trend will be $P \sim B^2$ and will not be representative of the true dynamical law.

This issue can be made mathematically explicit in the simple case of an 'ecosystem' made of a single species following logistic growth:

$$\frac{dB}{dt} = rB\left(1 - \frac{B}{K}\right) = \underbrace{rB}_{P(\text{production})} - \underbrace{\frac{DB^2}{}}_{L(\text{internal losses})} \quad (9)$$

When multiple ecosystems follow the same equation with different parameters, they will reach different equilibria. To avoid confusing the variation within one ecosystem and between different ecosystems, we denote here the equilibrium values in each ecosystem k by $B^{(k)}$, $P^{(k)}$ and $L^{(k)}$ (which satisfy $P^{(k)} - L^{(k)} = 0$). We can imagine two scenarios that lead to different scalings across systems:

- If systems have the same $r^{(k)} = r$ but different $D^{(k)}$ (and hence different equilibria $B^{(k)}$), the relationship $P(B) = rB$ within each system imposes the linear relationship $P^{(k)} \sim B^{(k)}$ across systems,
- If $r^{(k)}$ changes across systems while $D^{(k)} = D$ is constant, the relation $L(B) = DB^2$ and the equilibrium condition $P^{(k)} = L^{(k)}$ within each system impose the quadratic relationship $P^{(k)} \sim (B^{(k)})^2$ (in other words, we have a perfect colinearity $B^{(k)} \sim r^{(k)}$ across systems).

This example highlights the importance of knowing which parameter (here r or D) is most system-dependent to predict the empirical cross-ecosystem scaling law, and to identify how it differs from the true within-ecosystem dynamical relationship $P(B) = rB$.

The same issues occur for all observational scalings, including the scaling of predation losses with prey and predator densities: if we try to fit the relationship $C_{12} = AB_1^{\beta}B_2^{\gamma}$ in Eq. 6, we may encounter the problem of correlations between attack rates and population densities. We now discuss how to address this problem in the context of an empirical estimation of β and γ.

Empirical analysis

The empirical identification of a relationship between predation losses and species densities such as

$$C_{12} \sim B_1^{\beta} B_2^{\gamma}$$

can be affected by two sources of error: the colinearity between the two variables B_1 and B_2, and the colinearity of either of these variables with other factors that may appear in the full expression of C_{12} (e.g. the attack rate A defined above).

The first problem is that the colinearity between B_1 and B_2 (Fig. 1d) may obscure their respective contributions to $C_{12} = C(B_1,B_2)$. We can overcome this difficulty by performing a commonality analysis, which is a statistical test based on variance partitioning. We use the function *regr* of the R package *yhat* to check the existence of suppression i.e. the distorsion of regression coefficients due to the colinearity between predictors (Ray-Mukherjee et al. 2014). This test shows the absence of suppression, allowing us to directly interpret the respective contributions of B_1 and B_2 to $C(B_1,B_2)$ below.

A more important difficulty stems from correlations with other parameters, as suggested in the previous section. If we suppose that, in each ecosystem k, predation losses follow

$$C^{(k)}(B_1, B_2) = A^{(k)} B_1^{\beta} B_2^{\gamma} \quad (10)$$

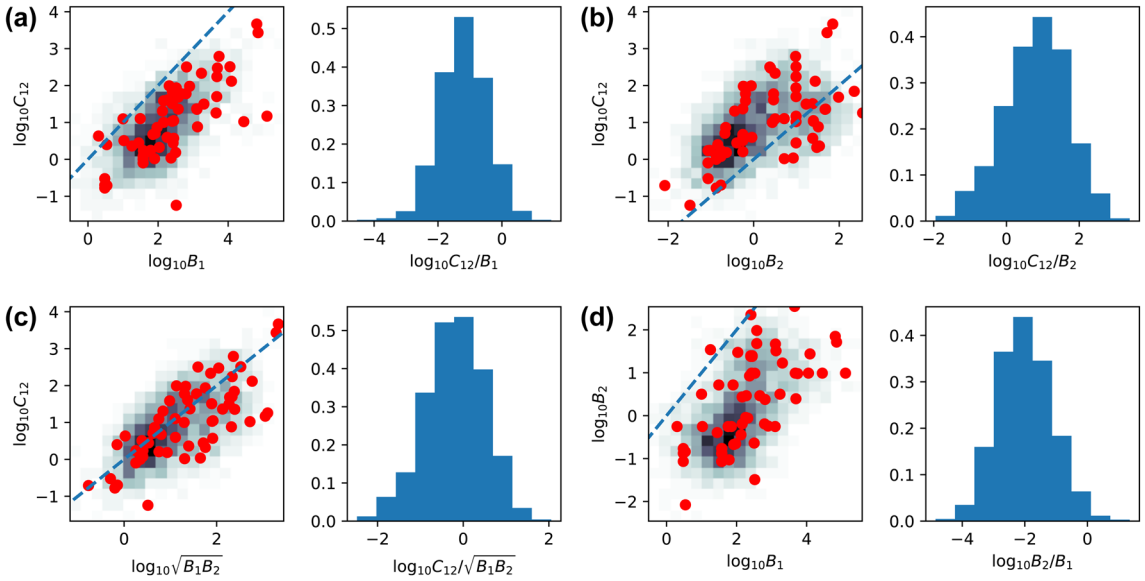

Figure 1. Empirical and simulated scaling relationships betwen biomass densities B_1 and B_2 and predation losses C_{12} in logarithmic scale. We show two panels for each pair among (a) C_{12} and B_1, (b) C_{12} and B_2, (c) C_{12} and $\sqrt{B_1B_2}$ and (d) B_2 and B_1. Left panels: each point corresponds to one study in our meta-analysis, and the dashed line represents the 1:1 relationship. The background color indicates the density of simulated realizations of our dynamical model, retaining only realizations that approximate the empirical distribution ('Dynamical model estimation' section). Right panels: histogram of ratio between the two quantities in our simulated ecosystems.

where we are given no information on the species-dependent parameter $A^{(k)}$, we can only estimate β and γ from a simple empirical fit if $A^{(k)}$ is weakly correlated with the observed values of B_1 and B_2. This could be the case if $A^{(k)}$ varies less between systems, or has less impact, than other factors that control B_1 and B_2, such as primary production or mortality (or factors ignored in our model, such as spatial fluxes, out-of-equilibrium dynamics and additional interactions).

We employ two distinct methods to identify the exponents β and γ in our proposed power-law scaling relationship.

The first approach is a direct fit, with the aim of minimizing residual variance: given that C, B_1 and B_2 span multiple orders of magnitude, any combination of these variables that exhibits much less spread suggests an interesting regularity, even though the precise values of the exponents may be incorrectly identified due to colinearities and should be interpreted with care.

The second approach is an attempt to account for at least some unknown factors that may undermine a naive parameter estimation. We focus on the dynamical food chain model (Eq. 2) and the power-law predation rate (Eq. 6). We then simulate this model for many random combinations of parameter values (including exponents, but also attack rate, growth rate, mortality, etc.). We only retain model realizations that give triplets (B_1,B_2,C) sufficiently close to those found in our empirical data, giving us a distribution of exponents compatible with this evidence, as well as an estimation of how other parameters may affect observed species densities and predation rates.

Direct fit

We note that the factor $A^{(k)}$ is not unitless. This may be problematic when fitting data collected at different scales. Following the discussion in Box 1, we propose to expand $A^{(k)}$ in a way that accounts for metabolic scaling and nonlinearity thresholds, i.e.

$$C^{(k)}(B_1,B_2) = a^{(k)} m_2 B_2 \left(\frac{m_1}{m_2}\right)^{\nu} \left(\frac{B_1}{B_{1,\min}}\right)^{\beta} \left(\frac{B_2}{B_{2,\min}}\right)^{\gamma-1} \qquad (11)$$

where m_2B_2 sets the dimensions of C and all other factors are dimensionless. In particular, $a^{(k)}$ is an ecosystem-dependent parameter that can be interpreted as a random effect. We will see in the Results section that many terms in this complex equation appear to have a negligible contribution, leading back to our simple theoretical expression (Eq. 6).

We have no direct measurement of the reference densities $B_{i,\min}$, which are necessary to construct dimensionless ratios, and which we interpret as thresholds for nonlinearity (saturation or interference). Therefore, we must make some assumptions on these values, guided by biological intuitions. The simplest possible assumption is that these thresholds vary independently of other parameters, and can be included into the random effect $a^{(k)}$. As a second option, if these density thresholds were proportional to individual body masses, $B_{i,\min} \sim w_i$, the relevant variables for our fit would be population densities N_i rather than biomass densities. A third option, $B_{i,\min} \sim 1/m_i$, would instead suggest focusing on

$E_i = m_i B_i$ which has commonly been interpreted as an 'energy' density (Damuth 1987). For each of these choices, the exponents ν, β and γ may then be identified by a least-squares linear regression in log space. To identify the correct definition of $B_{i,\min}$, we test all three possibilities, and ask which one leads to the best predictions, i.e. the lowest amount of residual variation in $a^{(k)}$.

Dynamical model estimation

Using our dynamical model (Eq. 2) with Eq. 5 and 6, we generate predator–prey pairs with different parameter values drawn from a broad prior distribution, and compute their equilibrium biomass densities B_1 and B_2 and predation losses C_{12}. We then retain only model realizations for which the three values (B_1, B_2, C_{12}) are close to those observed in our data. We repeat this process until we have retained 2500 model realizations, and use the parameter values of these realizations to compute a joint posterior distribution for all our parameters, in particular the exponents β and γ that we wish to identify.

For two species, our model has eight parameters, which we draw independently in each model realization. The exponents β and γ are drawn uniformly in the range [0,1.5] in order to confirm that they are expected to be less than 1 (the Lotka–Volterra or mass action limit). Other parameters are drawn uniformly on a log scale, over a span of 10 orders of magnitude: the attack rate $A \in [10^{-5}, 10^{5}]$, prey productivity $g_1 \in [10^{-4}, 10^{6}]$, predator mortality $\mu_2 \in [10^{-8}, 10^{2}]$ and prey and predator self-regulation $D_1, D_2 \in [10^{-5}, 10^{5}]$. Finally, the biomass conversion efficiency is drawn in the realistic interval $\varepsilon \in [10^{-2}, 1]$.

We retain only model realizations in which both species survive, and filter the remaining according to their similarity to empirical data. To do so, we train a Kernel density estimator (KDE, from the Python library *scikit-learn* using classes *GridSearchCV* and *KernelDensity*) on triplets $(\log_{10}B_1, \log_{10}B_2, \log_{10}C_{12})$ in the empirical data. We then compute the same triplet in model realizations, and its score s given by the KDE. We retain each model realization with probability $e^{\theta(s-s_{\max})}$, given $s_{\max}$ the highest score given among empirical triplets. We choose $\theta = 2$ as we find empirically that it gives the best agreement between simulations and data for the variance and range of B_1, B_2, C_{12} and their ratios.

Finally, we compute the posterior distribution of parameters, i.e. histograms of the parameter values found in accepted model realizations, and study their correlations with each other and with dynamical variables B_1, B_2 and C_{12}. For additional tests in Fig. 5 we ran the same procedure while restricting which parameters vary (sampling only g_1 and exponents β and γ, or keeping D_i or A_{12} constant) in order to demonstrate the relationship between scaling laws, discussed in the 'Links between statistical and dynamical laws' section.

Results

Meta-analysis of kill rates

Results from direct fit

The full expression to be fitted (Eq. 11) breaks down predation losses C_{12} into three different contributions: the observed species densities B_i raised to the exponents β and γ; the metabolic rates m_i, which are often assumed to define the time scale for predation processes; and the unknown typical density scales $B_{i,\min}$, which we interpret as thresholds for nonlinearity (e.g. the scale for interference or saturation).

Our first result is that there does not seem to be a systematic effect due to typical density scales $B_{i,\min}$. As explained in 'Direct fit' section, our main three choices for these parameters correspond to using biomass densities B_i, number densities N_i or 'energy' densities $E_i = m_i B_i$ as our fitting variables. To showcase these different options, we detail in Table 1 the residual standard deviation for various examples of power-laws involving these variables. These examples are only a few representative points in our systematic exploration of Eq. 11, but they illustrate our finding that number densities give the poorest results, while biomass or energy densities give comparable results. For simplicity, we then focus on biomass densities B_i, corresponding to the assumption that the reference density $B_{i,\min}$ is independent of body size or metabolism (This is consistent with assuming that the thresholds $B_{1,\min}$ and $B_{2,\min}$ are equal or proportional to the minimal sustainable population densities for prey and predators. Cross-species data from Hatton et al. (2015) and Stephens et al. (2019) suggest that the minimal numeric density is roughly inversely proportional to body mass, $N_{i,\min} \sim 1/w_i$. Therefore, $B_{i,\min} = w_i N_{i,\min}$ is expected to be size-independent, and exhibits no known link to metabolism.).

Our second result is the limited impact of metabolic rates on predation losses. From dimensional analysis (Box 1), we expected a baseline scaling $C_{12} < m_1$ or m_2. But we find that including m_i as a prefactor has no significant impact on any of our parameter estimates. Furthermore, irrespective of our choice of variable, our estimates for exponent ν in Eq. 11 are all of order $\nu \approx 0.1$, suggesting a weak and perhaps spurious dependence in metabolic rates. We therefore eliminate m_i

Table 1. Residual standard deviation for ratios of predation losses and biomass density B_i, population density N_i or 'energy' density $E_i = m_i B_i$. Figure 2 for a visualization of the residual variation with B_1/B_2 for the first three expressions. For the rightmost expression, we use the best-fit exponents $\beta = 0.47$, $\gamma = 0.30$, and see that this contributes only a small reduction of residual variation compared with the square root expression (second column). The three lowest residual variations are shown in bold.

Expression y	$\frac{C}{B_1}$	$\frac{C}{\sqrt{B_1 B_2}}$	$\frac{C}{B_2}$	$\frac{C}{N_1}$	$\frac{C}{\sqrt{N_1 N_2}}$	$\frac{C}{N_2}$	$\frac{C}{E_1}$	$\frac{C}{\sqrt{E_1 E_2}}$	$\frac{C}{E_2}$	$\frac{C}{B_1^{\beta} B_2^{\gamma}}$
std($\log_{10} y$)	0.90	**0.77**	0.97	1.6	1.5	1.5	0.93	**0.77**	0.9	**0.74**

from our Eq. 11. We performed a similar analysis (not shown here) using body masses w_i, with comparable results.

Given these two simplifications, we are left with the simpler relationship (Eq. 6) i.e.

$$C_{12} \sim A B_1^{\beta} B_2^{\gamma}$$

to be fitted. We find the best-fit exponents $\beta = 0.47 \pm 0.17$ and $\gamma = 0.30 \pm 0.19$. The limited extent of our dataset implies large uncertainty on the exact exponents, but they are starkly sublinear.

We notice that these exponents lay close to the line $\beta + \gamma = 1$, i.e. a simpler ratio-dependent model $C_{12} \sim B_2 (B_1/B_2)^{\beta}$ which we could have assumed for dimensional reasons (Box 1). If we impose this relationship by setting $\gamma = 1 - \beta$, we find a similar best-fit value $\beta = 0.51 \pm 0.12$. Due to the colinearity between B_1 and B_2 ($R = 0.56$, Fig. 1d), we might expect any model of this form to provide a comparable fit, ranging from $\beta = 1$ (donor dependent, Box 2) to $\beta = 0$ (consumer dependent). Nevertheless, our colinearity analysis strongly indicates $\beta \approx \frac{1}{2}$ as the most likely value. This is visualized by the fact that C/B_1 and C/B_2 both exhibit a residual variation in B_1/B_2 ($p < 10^{-6}$, $R = 0.61$ and $R = -0.52$ respectively, Fig. 2) whereas our best fit exhibits no residual variation ($p = 0.4$, $R = -0.08$), suggesting that neither strict donor nor consumer dependence prevails in our data.

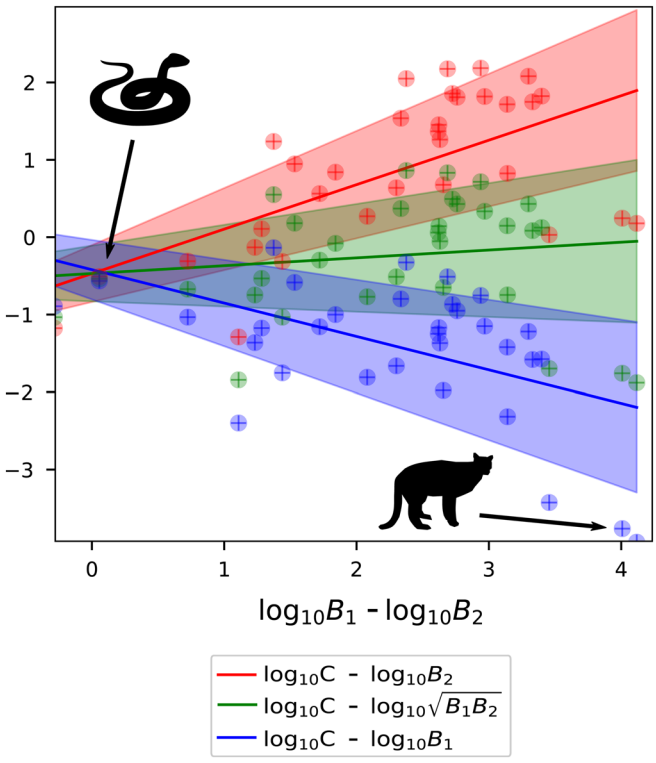

Figure 2. Residual variation with $\log_{10} B_1/B_2$ when assuming strict donor dependence ($C \sim B_1$), a symmetric square-root law ($C \sim \sqrt{B_1 B_2}$), or strict consumer dependence ($C \sim B_2$). Residues around the square-root law show no trend ($p = 0.4$, $R = 0.08$), and have minimal variance (Table 1).

Results from dynamical model estimation

We show in Fig. 3 the results of our second method of parameter estimation, described in 'Dynamical model estimation' section, which consists in simulating our dynamical model with random parameter combinations, and retaining those that produce densities and predation losses comparable to those of the data.

This second approach also supports the idea that $\beta + \gamma$ (whose distribution is centered close to 1) is significantly reduced compared to the mass action expectation $\beta + \gamma = 2$. However, we notice a stark asymmetry in the posterior

Box 2. Definitions

We introduce two sets of terms to distinguish:

- what sort of dependence is assumed for predation losses C, e.g. in our model (Eq. 6)

  donor-dependent predation A model where $C(B_1,B_2) = C(B_1)$, e.g. $\gamma = 0$
  consumer-dependent predation A model where $C(B_1,B_2) = C(B_2)$, e.g. $\beta = 0$
  ratio-dependent predation A model where $C(B_1,B_2) = B_2 C(B_1/B_2)$, e.g. $\beta + \gamma = 1$

- what are the dynamical outcomes of the balance between predation and internal losses

  regulated regime A solution of our model where each trophic level is mainly limited by self-regulation, as in logistic growth. If we increase the predators' individual consumption (attack rate A and exponents β and γ), more predators coexist at equilibrium.
  feedback regime A solution of our model with strong feedbacks between the two trophic levels (each level limits the other). From the predators' viewpoint, prey stocks are depleted, leading to competition for prey production. If we increase individual consumption, each predator uses up more of that flux, and fewer predators coexist at equilibrium.

These definitions attempt to avoid confusions surrounding the notions of bottom–up and top–down control, which often merge mechanisms (density-dependence) and dynamical outcomes. Intuitively, bottom–up control increases with β, top–down control increases with γ, and the feedback regime requires both types of control to be strong, creating 'antagonistic control' (Barbier and Loreau 2019). Such mutual limitation is shown in predator–prey cycles, or resource and apparent competition (Holt and Bonsall 2017).

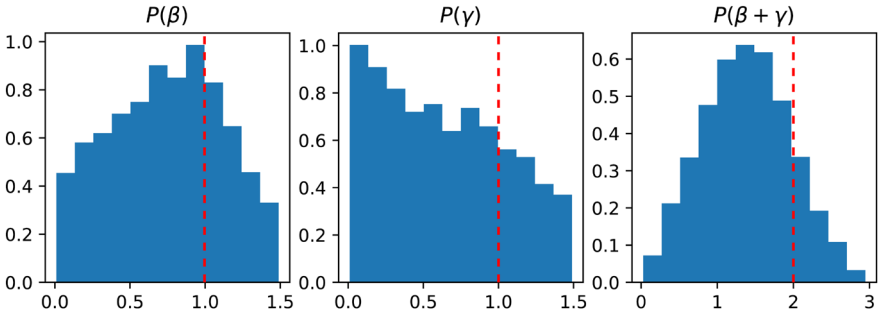

Figure 3. Posterior distributions of exponents β and γ in power-law predation rate (Eq. 6) for simulations selected to reproduce the empirical distribution of densities B_1 and B_2 and predation losses C_{12} (Fig. 1). The prior distribution was uniform over the interval [0,1.5]. The posterior distributions remain broad, showing that exponents are only weakly constrained by our empirical evidence (with almost no correlation between exponents, R = 0.11). The most likely values are β ≈ 0.9, γ ≈ 0 which approximate the classic model of linear donor-dependence (Box 2), while the median values are more symmetrical, β ≈ 0.8, γ ≈ 0.5 and hence β + γ ≈ 1.3. Both show significant departure from the mass action (Lotka–Volterra) hypothesis β = γ = 1 (dashed lines).

distributions of β and γ: the distribution of β has a mode below but close to 1, while the distribution of γ is strictly decreasing from 0. This might lend some credence to purely donor-dependent trophic fluxes, a hypothesis which lacked support in our direct fit approach above (Fig. 2).

We must note that this model exploration is still missing many other factors that may affect B_1 and B_2 and their relationship to C_{12}, such as non-equilibrium dynamics or interactions with other prey and predator species, among others. These factors may have a greater impact on predators, whose populations are typically smaller, slower to attain equilibrium and more easily perturbed. We could thus expect that measured predator abundances are less strictly related to C_{12}. This decorrelation may be sufficient to explain the apparent bias toward small γ. We discuss below the hypothesis that our results are mainly driven by an artificial donor-dependence imposed by the scale of observation in the data.

Comparison with a classic functional response

We recall that the functional response designates the predation rate per predator (either per individual or per unit biomass, depending on studies), and thus corresponds here to C_{12}/B_2. The DeAngelis–Beddington (DAB) model (8), or Holling type 2 with predator interference, can be fitted to our data, but while it may be useful as a mechanistic model for a single system (Barraquand 2014), it is unsatisfactory in our macro-ecological approach.

This expression faces the following problem: the thresholds for prey saturation H and predator interference I are not only particular to each pair of species (e.g. via their body sizes (Pawar et al. 2012)), but they also depend on the spatio–temporal structure and scale of each system. For instance, a day-long experiment in a closed arena may reveal saturation with prey density due to predator handling and satiety. But over a month in an open landscape, a different saturating effect could appear due to prey refuges. If we measure multiple systems at different scales, each may have a different saturation constant, and we cannot fit them all using the same saturating function with fixed, or even independently varying, values of H and I. We tried to construct some plausible expressions for system-dependent H and I using other known parameters for each system (e.g. body sizes, metabolic rates and spatial extension), but could not find a successful approach. Assuming H and I to be constant instead, we perform a fit and find (Supporting information) that almost all predator–prey pairs are in the saturated part of the function, i.e. $HB_1 + IB_2 \gg 1$. This suggests that the DAB model best approximates the data in the limit where it becomes linear in either B_1 or B_2, which is also a special case of our power-law model.

Furthermore, we show in the Supporting information that the colinearity $B_1 \sim B_2$ can make it difficult to differentiate between an additive law, $HB_1 + IB_2$ and a multiplicative law with exponents adding up to one, $B_1^{1-\beta}B_2^{\beta}$, in the denominator of the functional response. This has been put forward as an important criticism of the Cobb–Douglas production function (Felipe and Fisher 2003) which resembles our power-law model (Eq. 6). But we find here that prey and predator appear to be both limiting. This requires a fine-tuning of the ratio of handling time to interference, H/I, so that HB_1 and IB_2 are comparable in magnitude. This is found in our best fit of the DAB model (Eq. 8) but is difficult to justify mechanisticially, whereas the same reality may be more clearly and simply encapsulated by our ratio-dependent (β + γ ≈ 1) expression with β < 1.

Theoretical properties and consequences of empirical exponents

Population sizes

We consider two trophic levels, and investigate equilibrium predator density B_2^* in Fig. 4a as a function of both exponents β and γ. We observe two distinct regimes: there is only one stable equilibrium throughout the parameter space, but it is dominated either by species self-regulation, or by trophic regulation.

These regimes can be understood by first assuming that self-regulation can be neglected at both levels. In that case, our dynamical model (Eq. 2) with the power-law expression (Eq. 6) has the equilibrium solution (Supporting information)

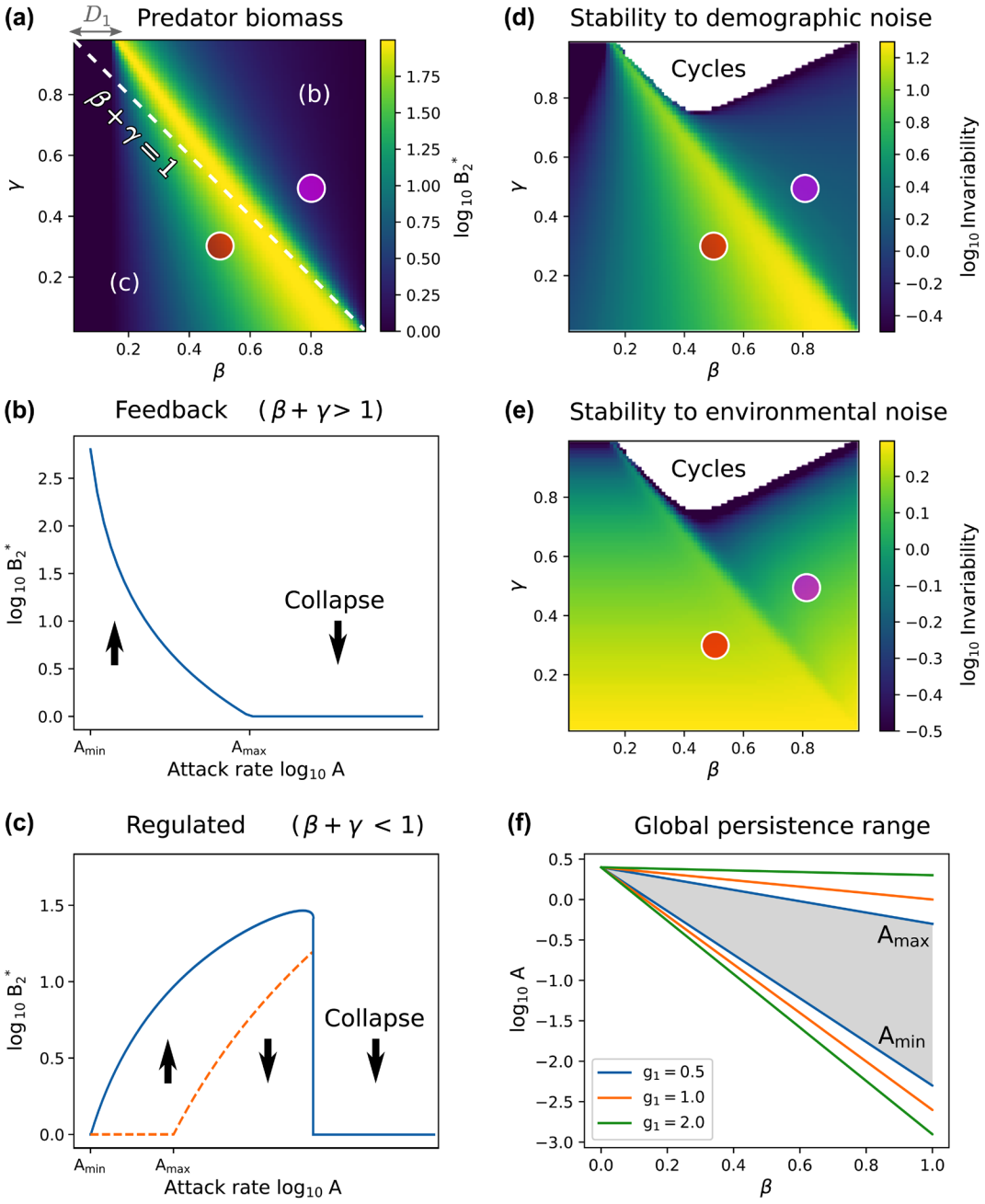

Figure 4. Predator abundance and persistence in our dynamical model ($D_i = 10^{-3}$ at both levels, $g_1 = 1$, $\mu_2 = 2$, $\varepsilon = 0.8$, setting the extinction threshold at B_i=1). (a) Predator biomass density B_2^* (in log scale) varies with exponents β and γ in the power-law predation rate (Eq. 6). It is maximized on a boundary separating two different regimes (b and c). This boundary is close to the dashed line $\beta + \gamma = 1$, but deviates due to self-regulation D_i. (b) For $\beta + \gamma > 1$, the resource is depleted by predation (feedback regime in Box 2), and predator population decreases with attack rate, going extinct at A_{max}. (c) For $\beta + \gamma < 1$, predator biomass (solid line) increases with attack rate, since the resource is mainly limited by its own self-regulation. The predator may survive if $A > A_{min}$, but an unstable equilibrium (dashed line) emerges at $A > A_{max}$, under which populations can go extinct. (f) For the predator to persist in both regimes and for all initial conditions, we must have $A_{min} < A < A_{max}$ (shaded region). This interval expands with higher β (less saturation) and prey growth g_1. (d–e) Predator invariability (1/coefficient of variation, Supporting information) in response to (d) demographic fluctuations and (e) environmental perturbations on the predator. For large γ and $\beta < 1$, the equilibrum can be unstable and replaced by limit cycles. This area is left blank, but invariability remains well-defined in simulations. (a, d, e) The red dot shows the exponents from direct regression $\beta \approx 0.5$, $\gamma \approx 0.3$, and the purple dot shows median values from our dynamical model fit, $\beta \approx 0.8$, $\gamma \approx 0.5$.

$$B_1^* \approx \left(\frac{g_1^{1-\gamma} (\mu_2 / \varepsilon)^{\gamma}}{A_{12}} \right)^{\frac{1}{\beta+\gamma-1}} \quad B_2^* \approx \left(\frac{g_1^{\beta} (\mu_2 / \varepsilon)^{1-\beta}}{A_{12}} \right)^{\frac{1}{\beta+\gamma-1}} \quad \text{if } D_i \to 0 \qquad (12)$$

where we see that $\beta + \gamma = 1$ leads to a singularity, meaning that self-regulation cannot be neglected for these exponents.

The first regime is found when $\beta + \gamma > 1$, and we call it the *feedback* regime (Box 2 and Fig. 4b). In this case, the solution (Eq. 12) is a good approximation at low self-regulation (small D_i). We notice that this solution has two counter-intuitive properties: predator biomass B_2 decreases with attack rate A_{12} and exponents β and γ, and increases with predator mortality μ_2 (if there is saturation, $\beta < 1$). This is because prey stocks are brought to low levels, so predators simply divide between themselves the flux of prey production: the more each predator consumes per capita, the fewer predators can coexist. As we discuss below, this inverse relationship between individual fitness (high attack rate, low mortality) and population abundance has been demonstrated in various models and called the 'hydra effect' (Abrams 2009, Schröder et al. 2014).

If $\beta + \gamma < 1$, the solution without self-regulation (Eq. 12) becomes unstable. In the stable equilibrium, the biomass of prey will be mainly determined by their self-regulation i.e. $B_1^* \approx g_1 / D_1$, leading to what we call the regulated regime (Box 2 and Fig. 4c). In that case, predator biomass

$$B_2^* \approx \left(\frac{\varepsilon A_{12}}{\mu_2} \right)^{\frac{1}{1-\gamma}} \left(\frac{g_1}{D_1} \right)^{\frac{\beta}{1-\gamma}} \qquad (13)$$

increases with attack rate and with exponents β and γ. The fact that the previous equilibrium (Eq. 12) is unstable reveals a type of Allee effect: if initial prey levels are below a threhsold, predators will consume all the prey (consumption will decrease too slowly to adjust to the falling resource level) then collapse.

We show in Fig. 4 that predator abundance is maximized at the boundary between these two regimes. This boundary lies close to the line $\beta + \gamma = 1$, where predation losses scale as

$$C(B_1, B_2) \sim B_1^{\beta} B_2^{1-\beta}$$

which is close to the exponents suggested by our meta-analysis. We however note that the regime boundary moves away from this line as we decrease attack rates A_{12} and increase self-regulation D_i at both levels. For sufficiently high self-regulation, even Lotka–Volterra dynamics can enter the regulated regime, which can be interpreted as classic bottom–up control (Barbier and Loreau 2019).

The overarching pattern is that the predator density first increases with attack rate A_{12} and exponents β and γ, when predation losses are still negligible for the prey, up to the regime boundary described above. Past this point, faster consumption leads to significant resource depletion and a drop in predator population (Loreau 2010), as competition increases more than growth.

Dynamical stability

We also observe how predation rate exponents affect the stability of predator populations. Figure 4d–e represents the invariability (inverse of the coefficient of variation over time) of predator abundance, computed in two scenarios: demographic stochasticity, where fluctuations (arising from birth and death processes) are proportional to $\sqrt{B_2}$, and environmental perturbations which affect the predators proportionally to their abundance B_2 (Arnoldi et al. 2019). Other scenarios and more stability metrics (including asymptotic resilience) are represented in the Supporting information, and show qualitatively similar patterns.

We make three main observations. First, the optimal parameter values for stability depend on the perturbation scenario (e.g. demographic or environmental noise) and the choice of stability metric, as having a larger abundance leads to higher stability in some metrics (Arnoldi et al. 2019). It is therefore important to know which scenario and metric are relevant for empirical dynamics, and different ecosystems may possibly have different optima. Second, all the cases studied here display a ridge of increased predator stability at the maximum of its abundance, close to the transition line $\beta + \gamma = 1$, and a drop in stability right after this ridge. Third, while abundance depends almost symmetrically on β and γ, and is maximized close to the transition between regimes, stability favors systems closer to donor-dependence. Moving toward larger β along the line $\beta + \gamma = 1$ reduces the likelihood of cycles and widens the region of parameters with high stability both to demographic and environmental noise (Fig. 4d–e). More generally, stability to environmental perturbations can be improved by having lower γ than what would maximize abundance (i.e. going toward the bottom of Fig. 4e).

Scaling of biomass and production across levels

Previous literature has reported scaling laws between biomass and production within one trophic level,

$$P_i \sim B_i^{\delta} \qquad (14)$$

and between biomasses at different trophic levels (Hatton et al. 2015)

$$B_{i+1} \sim B_i^{\alpha} \qquad (15)$$

As discussed in Barbier and Loreau (2019), neither of these laws can arise for more than two levels in a classic Lotka–Volterra model without self-regulation ($\beta = \gamma = 1$, $D_i = 0$).

In the following, we illustrate how such empirical scalings can emerge from underlying dynamical relationships, and how the measured exponents will depend on which parameters drive the cross-ecosystem variation in predator and prey density. There are only two ways in which scaling laws can

hold consistently across multiple trophic levels: either they are imposed by a narrow class of density-dependence for predation rates, or they originate from an equilibrium balance between trophic processes and other losses.

The first possibility requires internal losses to be negligible, i.e. $L_i = 0$ in Eq. 2, and predation to be strictly donor-dependent or consumer-dependent ($\gamma = 0$ or $\beta = 0$). The predation density-dependence then completely determines the scaling between production and biomass,

$$P_i \sim B_i^{\beta} \quad \text{or} \quad P_i \sim B_{i-1}^{\gamma} \tag{16}$$

and since $L_i = 0$,

$$P_{i+1} = \varepsilon P_i \Rightarrow B_{i+1} \sim B_i \tag{17}$$

which entails a strict proportionality between predator and prey biomass (exponent $\alpha = 1$). This has been widely discussed by proponents of the ratio-dependent functional response (Arditi and Ginzburg 2012), and the existence of such proportionality laws was put forward as evidence of donor control. But since we find nonzero β and γ, this possibility is excluded by our data.

The second possibility arises in our model with a power-law predation rate (Eq. 6). Following the Supporting information, we illustrate our reasoning in the case where the scaling $P_i \sim B_i^{\delta}$ emerges from the density-dependence of internal losses. If we assume that all three terms $C_i \sim L_i \sim P_i$ in the dynamics (Eq. 2) remain of comparable magnitude at equilibrium (i.e. that a finite fraction of biomass is always lost to predation and to internal losses both), the expression of L_i can indeed impose a scaling between production and biomass:

$$L_i = D_i B_i^{\delta} \quad \text{and} \quad L_i \sim P_i \Rightarrow P_i \sim B_i^{\delta} \tag{18}$$

(this requires that the cross-ecosystem variation in densities B_i be mostly due to other parameters, with the exponent δ and coefficients D_i varying little between systems, 'Links between statistical and dynamical laws' section, but a parallel argument can be made when other parameters are held constant). For instance, we have $\delta = 1$ for individual mortality, and $\delta = 2$ when a self-regulating process, such as intra-specific competition or pathogens, is the main contributor to internal losses. We show in the Supporting information that a relationship then emerges between the exponents defined in Eq. 14 and 15 and the predation rate exponents

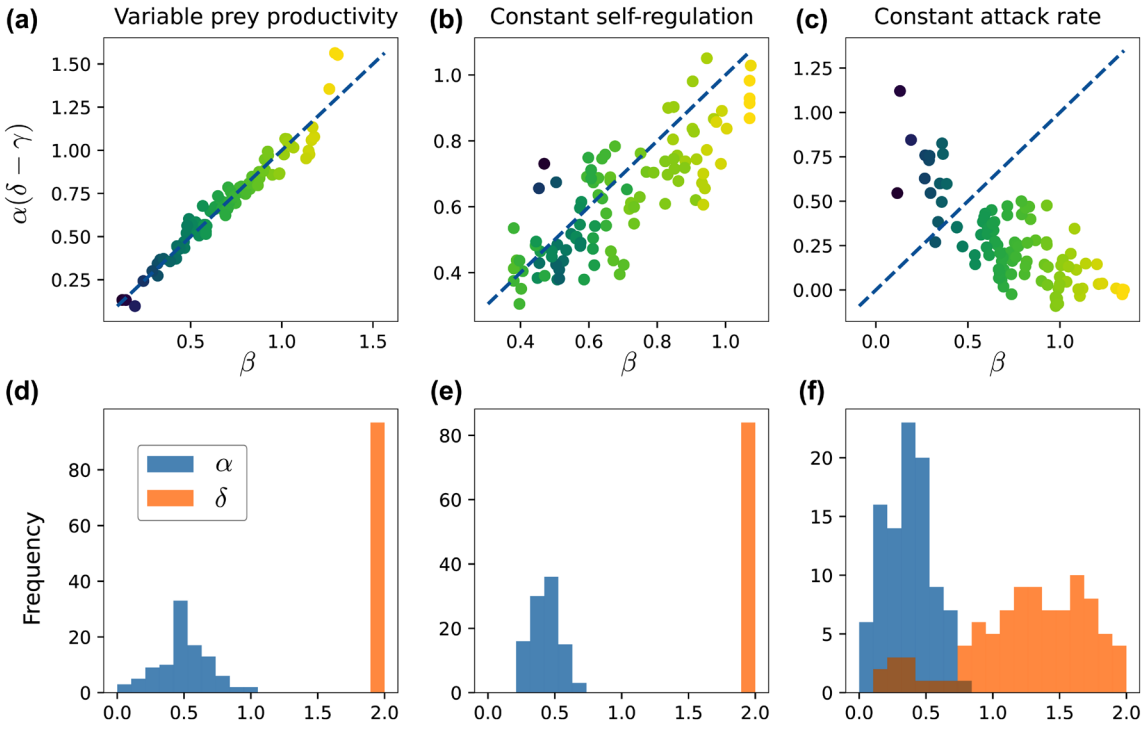

Figure 5. Numerical test of the theoretical relation between scaling laws, $\alpha(\delta - \gamma) = \beta$ in (Eq. 19), derived in the example of constant self-regulation coefficients D_i across ecosystems. We vary exponents β and γ in the power-law predation rate, and perform regressions to compute the exponents of empirical scaling laws: α for the predator–prey density scaling, and δ for the prey's production-density scaling. (a, d) Simulations that differ only through their prey productivity g_1 and exponents β and γ. (b, e) Simulations where all parameters vary except self-regulation coefficients D_1 and D_2. (c, f) Simulations where all parameters vary except attack rate A_{12}. We see that the predicted scaling laws depend on which parameter is expected to vary most, so that different calculations may need to be performed depending on which features play the largest role in differentiating observed ecosystems.

$$\alpha(\delta - \gamma) = \beta \quad (19)$$

We illustrate this relationship numerically in Fig. 5, using the simulated runs discussed in 'Dynamical model estimation' section where some parameters are kept constant. We group simulation runs into bins, based on the value of their exponents β and γ, then compute the scaling exponents α and δ within each bin, by running regressions for the scaling laws Eq. 14 and 15. We find that our prediction (Eq. 19) is successful when self-regulation is constant, and especially when ecosystems differ only by their prey productivity. On the other hand, when self-regulation varies largely, colinearities between parameters and equilibrium densities confound the empirical scaling laws, as discussed in 'Links between statistical and dynamical laws' section, and lead to a violation of this prediction. Similar calculations can however be performed for any assumption about which parameter is mainly responsible for cross-ecosystem differences in predator and prey density.

Commonly assumed scaling exponents for biomass and production are $\alpha = \delta = 1$, i.e. simple proportionality between predator and prey biomass, and between production and biomass at each level. These relations are used in various mass-balanced models (Pauly et al. 2000) or theory on biomass pyramids (Borgmann 1987). They entail $\beta = 1 - \gamma$, meaning that the relationship between predation losses and biomasses would be the ratio-dependent expression $C_{12} \sim B_2(B_1/B_2)^{\beta}$ which we have discussed in previous sections.

Discussion

The dependence of predation rates on predator and prey densities is a crucial component of trophic ecology, that has a considerable impact on predator–prey dynamics (Holling 1965). Long-standing debates have opposed advocates of various forms of functional response (predation rate per unit predator), such as prey-dependent or ratio-dependent expressions (Arditi and Ginzburg 1989, Abrams 2015). The current consensus seems to be that there is no correct universal expression; rather, different functional responses are appropriate in different settings, and they should be derived mechanistically for each studied ecosystem (Barraquand 2014, Abrams 2015).

From a macro-ecological point of view, however, what matters is how the predation rate scales up across several orders of magnitude in abundance, body size and area. Experiments typically measure predation rates for a given pair of species, and how they respond to varying the number of prey and predator individuals, on a short time scale and in an enclosed space. Here, we used kill rates recorded in the field to estimate how predation rates over long times (e.g. a year) vary between species (mainly terrestrial vertebrates) and across much larger spatial scales.

Our empirical analysis points to a phenomenological power-law, which differs from commonly-studied mathematical expressions. If this law does hold dynamically within each ecosystem, it may have striking theoretical implications. The empirical exponents fall close to the boundary between two qualitatively distinct dynamical regimes (approximately the line $\beta + \gamma = 1$). This boundary has two properties in our food chain model: predator abundance is maximized, and simple allometric scaling laws appear between different ecosystem functions and between trophic levels. We may then ask whether these two important macroscopic properties arise accidentally from a predation density-dependence shaped by other constraints, or whether this density-dependence is in fact selected for its dynamical consequences.

Is the empirical density-dependence an artefact of donor-dependence?

Our theoretical model suggests that both saturation and interference can lead to similar qualitative consequences for many ecosystem properties. Yet, two main empirical results suggest that reality is closer to classic donor-dependence, i.e. assuming that trophic fluxes are only determined by the amount of resource, and in turn determine the abundance of consumers, and not the reverse. The first clue is the fact that C_{12}/B_1 is largely below 1, and the second is that exponent γ is consistently lower than β. As discussed previously, the precise values of these exponents are weakly constrained empirically and could be confounded by unknown latent factors, disguising an underlying process where $\beta = 1$ and $\gamma = 0$.

To properly assess the value of these clues, it is important to recognize that donor-dependence is not a necessity. Predation losses are in principle limited not by standing biomass, but by production,

$$C_i \lesssim P_i$$

which can be much larger than standing biomass. For instance, a Lotka–Volterra model with a classic biomass pyramid $B_{i+1} \sim B_i$ would predict the predation and production of all consumers to scale quadratically with biomass, as $B_{i+1}B_i \sim B_i^2$. In other words, more and more productive systems would exhibit more and more predation, but populations would only increase as the square root of these fluxes, and prey density B_1 would not represent a bound on predation. A supralinear scaling of production and losses with biomass is not implausible. Analogous relationships have been proposed in economic systems, with empirical exponents ranging from 1.16 (economic growth as a function of city size (Bettencourt et al. 2007)) to 1.6 (stock trading rate as a function of number of shares (Barbier and Lee 2017)). We could also invoke empirical facts that have been interpreted as evidence for the Allee effect (Kramer et al. 2009), since this effect assumes that per-capita growth rate increases with density, and hence, that production P_i is supralinear with biomass B_i.

There is, however, an important reason for expecting donor-dependence to prevail, especially at large spatial and temporal scales where many ecological processes are

aggregated: the possibility of a bottleneck in the dynamics. In various ecological contexts, only a fraction of possible prey (or predators) are available for predation events. This can include the existence of prey refuges in space (Poggiale et al. 1998), or the specialization of predators on particular age classes. The rate at which prey become available can be the limiting factor in the overall predation intensity, which therefore becomes purely donor-dependent. For example, if predators target prey of age one and above, these prey must have appeared in the previous year's census, imposing an insuperable bound $C_i < B_i$ (with a year's delay, ignored under equilibrium assumptions).

The evidence for or against this possibility is unclear here. In most of the data that we study, C_{12} is sufficiently small compared with B_1 that it could still plausibly increase with predator abundance, and there is no systematic preference for mature prey. On the other hand, our estimate of B_1 might miss other factors (such as refuges) limiting prey availability, as we discuss next. While a broader analysis across taxonomic groups, timescales and life histories would be needed to test for possible artefacts such as those suggested above, our provisional conclusion is that this empirical scaling of predation with densities is indeed meaningful, and goes beyond restating the classic donor-dependence hypothesis.

Is this density-dependence a consequence of biological constraints?

Nonlinear predation rates, with saturation and interference, are generally assumed to be imposed by a broad range of microscopic or mechanistic factors (physiology, behavior, spatial structure, individual tradeoffs between competition and consumption, etc). In various ways, these factors limit the space or time available for encounters, leading to less predation than under mass action.

The most immediate candidate mechanism to explain a pattern that holds across ecosystems and scales is spatial structure. For instance, local prey refuges have been proposed as a classic explanation for a donor-dependent (Poggiale et al. 1998) or DeAngelis–Beddington response (Geritz and Gyllenberg 2012). More generally, spatial structure has been shown to lead to power-law-like density-dependence of predation in agent-based or spatially explicit simulations (Keitt and Johnson 1995, Barraquand 2014). But this seems to allow a wide range of possible exponents, and therefore, it does not provide an unequivocal explanation for our observations.

A predation rate $C_{12} \sim \sqrt{B_1 B_2}$ ($\beta, \gamma \approx \frac{1}{2}$), similar to our measurements, could be imposed by spatial structure in two dimensions, if prey and predators occupy almost mutually exclusive regions and only meet at the boundaries (given that the periphery of a region scales like the square root of its area). This could happen due to local prey depletion by predators, a plausible explanation although it requires very strong negative correlations in space (Sjödin et al. 2015), and would predict a different scaling in three-dimensional settings (Pawar et al. 2012) which remains to be tested.

We cannot conclude, based on our data alone, that spatial heterogeneity is the main driver of our empirical predation density-dependence. Spatially explicit data may be necessary to test this hypothesis. If spatial structure does not impose an exponent, but allows a range of possibilities, it could provide the means through which predators and prey organize to achieve a certain density-dependence, that then has selective value for other processes (Pepper and Smuts 2001, Goodnight et al. 2008).

Can this density-dependence emerge from selection?

The mathematical expression and exponents found here are close to those which theoretically maximizes predator abundance and some metrics of stability. Yet this comes at an apparent cost to the individual predator, which consumes less here than under a classic Lotka–Volterra (mass action) scenario. We recall the so-called hydra effect (Abrams 2009, Schröder et al. 2014), a counter-intuitive but common phenomenon in resource-based dynamics: decreasing the fitness of individual consumers, e.g. increasing their mortality or reducing attack rates, can lead to larger populations in the long run, when this reduces competition more than it reduces growth. We showed that a similar effect applies here to consumptive saturation and interference, as represented by the power-law exponents β and γ in the predation rate. Maximal predator abundance is reached for exponents close to the relationship $\beta + \gamma = 1$, which holds approximately in data (More precisely, predator abundance is maximized at the boundary between two dynamical regimes, which is given by $\beta + \gamma = 1$ when species self-regulation is low, but moves toward higher exponents as we increase self-regulation and can be seen in Lotka–Volterra models (Barbier and Loreau 2019)).

This resonates with long-standing debates in ecology and evolution, in particular the group selection controversy (Wilson 1983) and its accounts of selection for population abundance (Wright 1945) or persistence (Wynne-Edwards 1962). Should we conclude here that consumption rates are selected to optimize population-level properties? And would this optimization require population-level selection, or can it arise strictly at the individual level? We now show that these are valid possibilities in our setting.

A first possibility is that our proposed density-dependence is outcompeted at the individual level, but selected at the population level, due to some positive consequences of having larger abundances. Extending our model to include simple adaptive dynamics of attack rate and scaling exponents, we indeed find that this dependence is dominated by other strategies (Supporting information). We observe maladaptive evolution: mutants with ever faster consumption will outcompete and replace residents, reaching ever lower equilibrium abundances, up until the point where the predators go extinct. A classic solution is to invoke competition between groups in a spatial setting (Wright 1945, Wilson 1983), as a larger group can send out more propagules and will often disperse faster (Haond et al. 2018). These intuitions pervade a

large literature on the evolution of 'prudent' predation strategies through group selection, also known as the milker–killer dilemma (Van Baalen and Sabelis 1995, Pepper and Smuts 2001, Pels et al. 2002, Goodnight et al. 2008).

A less obvious possibility is that our predation density-dependence is favored even at the individual level, as a result of direct competitive interactions. The dominance of faster consumers relies on the assumption that competition takes place only through resource consumption. In the presence of other competitive interactions that are not tied to resource levels, a larger standing population can resist invasion both by mutants and by other species. We suggest in the Supporting information that, for the resident population to be evolutionarily stable, this non-consumptive competition must induce higher mortality in individuals that search for more resources, regardless of their success. This feature seems plausible for territorial behavior and aggression as widely displayed by higher vertebrates (as an illustration, lions are both outliers in our dataset, since they display lower consumption rates than the general trend (Supporting information), and are a major cause of mortality among other carnivores (Hayward et al. 2007). These two features together may indicate a counter-intuitive predator strategy, which involves both consuming less prey and spending more time in non-consumptive competition, leading to and benefitting from population maximization.), but could also be induced e.g. by allelopathy in other organisms. Under these conditions, slow consumers can avoid being overtaken by fast consumers, even within a single population.

As a further perspective, all our arguments so far have taken the viewpoint of the predator's strategy and abundance, despite the fact that our empirical results suggests a roughly equal role of predator and prey density in limiting predation. Our best-fit exponents situate real systems close to the limit between a regime where prey suffer from predation, and a regime where they are mainly self-regulated. It is thus possible that prey strategies, or a balance between prey and predator selective pressures, are at play.

We conclude that selection on the predation rate exponents to maximize population size can easily arise in variations of our model, provided that we include non-consumptive processes (from dispersal to aggression). Some of these explanations involve competition between populations, while others take place within a single population, but all favor strategies that maximize predator abundance.

Can this density-dependence explain other power-law relations between ecosystem functions?

Relations between production and biomass, and between predator and prey densities are widely assumed and observed to take linear or power-law forms (Borgmann 1987, Hatton et al. 2015). Yet, we have shown that such relations do not emerge universally from arbitrary dynamical models. They require particular ecological conditions, where internal losses L_i within trophic level i are comparable to, or larger than, predation losses C_i (both in their magnitude and in their density-dependence). For instance, in a Lotka–Volterra model, strong density-dependent self-regulation within a trophic level is required to observe linear (isometric) relations between different functions and between levels, creating classic biomass and energy pyramids (Barbier and Loreau 2019). Alternatively, exponents $\beta+\gamma=1$ in our proposed expression recover the same linear relations and pyramids. When these conditions are not satisfied and predation losses are larger, the predator–prey dynamics can enter a feedback regime (Box 2) in which prey stocks are exhausted and may not follow any scaling relationship to either prey productivity or predator stocks, a property which has already been proposed as evidence for top–down control of prey by predators (Ripple and Beschta 2012).

A recent meta-analysis by Hatton et al. (2015) found sub-linear scalings of production with biomass (with exponent α) and of predator density with prey density (with exponent δ), following $\alpha \approx \delta \approx \frac{3}{4}$, reminiscent of metabolic allometry. Assuming that this cross-ecosystem law also holds dynamically within one system, so that our model results apply, this requires strong interference and saturation, $\beta+\gamma < 1$. The empirical evidence is too weak to decide whether $\beta+\gamma \approx 1$ (leading to isometry) or $\beta+\gamma < 1$ (leading to allometry), but both possibilities fall within the range of our estimates.

In summary, the existence of well-defined scaling laws across trophic levels, between ecosystem functions such as biomass and production, is less self-evident than it may appear. We suggest here that some empirically-supported laws might be secondary consequences of the mechanisms that determine our phenomenological predation density-dependence.

Conclusions

We have shown that the intensity of predation across a range of spatial scales and species can be modeled as a power-law function of both consumer and resource densities, that deviates strongly from the mass action (Lotka–Volterra) assumption. Density-dependence at these various scales may be driven by very different mechanisms, from individual behavior to population structure, all the way to spatial fluxes and landscape heterogeneity. Similar phenomena, such as prey saturation and predator interference, may nevertheless emerge from these different causes.

Amidst the vast literature on predation rates and functional responses, our choice of a phenomenological power-law model is motivated both empirically and by the fact that this law is scale-free. By contrast, many classic models contain a characteristic scale, such as a saturation threshold, and thus cannot retain the same parameters across multiple scales. When prey- and predator-dependence exponents sum to one, we recover a ratio-dependent functional response (Arditi and Ginzburg 2012), and classic donor control as a special case. Our empirical estimates are also compatible with a more symmetrical expression where predator and prey are roughly equally limiting, leading to an unusual square root expression. This model is reminiscent of the Cobb–Douglas

production function in economics (Cobb and Douglas 1928), which similarly arises in a macroscopic context, and is also disputed as either a salient empirical fact or a simple consequence of colinearity and aggregation (Felipe and Fisher 2003). Nevertheless, the main observation in both fields is that two factors – labor and capital, or consumers and resources – are co-limiting, so that doubling the output (here, yearly consumption) requires doubling each of the two inputs.

Nevertheless, scaling laws measured across ecosystems do not always hold dynamically within a single ecosystem (Hatton et al. 2019): other latent variables could differ between ecosystems, altering the relationship between predation and abundances that we would observe locally. Further work should employ data on temporal change to test whether our proposed expression truly applies to the dynamics of an ecosystem. Our results are also limited by the fact that we consider only one interaction at a time, as we generally lack data for other prey and predators interacting with our focal species. Our empirical investigation should therefore be extended to other taxonomic groups, and confronted to experimental evidence, to pave the way for a deeper understanding of the emergent density-dependence of total predation rates at macro-ecological scales.

Speculations

Should our phenomenological cross-ecosystem law be verified dynamically within each ecosystem, we have shown theoretically that the estimated values of the exponents have important implications for trophic dynamics. In particular, these values are close to maximizing predator population density and some measures of stability. Speculatively, this could reflect a cross-scale selection pressure acting upon consumption rates. While selection for abundance or stability is far from a given, we noted that it could be supported by non-consumptive competition (e.g. territorial exclusion or allelopathy), which itself appears surprisingly ubiquitous across forms and scales of life. This type of competition can indeed prevent the dominance of smaller populations of faster consumers, and may open a path for the evolution of strategies that limit predation to maximize predator abundance.

The observed density-dependence could also arise from prey strategies and refuges. While the literature on functional response has generally focused on the predator's viewpoint, we expect that a paradigm shift toward a more equal treatment of predator and prey strategies (as in parasite–host systems), and toward a more inclusive view of consumption-limiting mechanisms, including population and spatial structure, may be needed to truly understand trophic dynamics from the individual to the ecosystem scale.

We hope that future studies can address two fundamental questions: 1) whether the predation density-dependence that we observe stems purely from aggregation or from other ecological phenomena, and 2) whether some universal principle, such as selection for larger populations, could explain this density-dependence and, through it, the emergence of other widespread macro-ecological scaling laws.

Data accessibility statement

The dataset is available at <https://doi.org/10.6084/m9.figshare.13473102.v1>, with metadata and additional information in the Supporting information.

Acknowledgements – We thank F. Barraquand, I. Hatton and J. Prunier, as well as the PCI Ecology reviewers G. Barabás and L. Berec and recommender S. Suweis, for many helpful comments.
Funding – This work was supported by the TULIP Laboratory of Excellence (ANR-10-LABX-41) and by the BIOSTASES Advanced Grant, funded by the European Research Council under the European Union's Horizon 2020 research and innovation programme (666971).
Conflicts of interest – The authors declare that they have no financial conflict of interest with the content of this article.

Author contributions

Matthieu Barbier: Conceptualization (equal); Data curation (supporting); Formal analysis (lead); Investigation (equal); Methodology (equal); Supervision (equal); Validation (equal); Visualization (lead); Writing – original draft (lead); Writing – review and editing (equal). **Laurie Wojcik**: Conceptualization (equal); Data curation (lead); Investigation (equal); Methodology (equal); Writing – original draft (supporting); Writing – review and editing (equal). **Michel Loreau**: Conceptualization (equal); Funding acquisition (lead); Project administration (lead); Supervision (equal); Validation (equal); Writing – review and editing (equal).

References

Abrams, P. A. 2009. When does greater mortality increase population size? The long history and diverse mechanisms underlying the hydra effect. – Ecol. Lett. 12: 462–474.
Abrams, P. A. 2015. Why ratio dependence is (still) a bad model of predation. – Biol. Rev. 90: 794–814.
Abrams, P. A. 2019. How does the evolution of universal ecological traits affect population size? Lessons from simple models. – Am. Nat. 193: 814–829.
Aljetlawi, A. A. et al. 2004. Prey–predator size-dependent functional response: derivation and rescaling to the real world. – J. Anim. Ecol. 73: 239–252.
Arditi, R. and Ginzburg, L. R. 1989. Coupling in predator–prey dynamics: ratio-dependence. – J. Theor. Biol. 139: 311–326.
Arditi, R. and Ginzburg, L. R. 2012. How species interact: altering the standard view on trophic ecology. – Oxford Univ. Press.
Arnoldi, J. F. et al. 2019. The inherent multidimensionality of temporal variability: how common and rare species shape stability patterns. - Ecol. Lett. 22: 1557-1567.
Barbier, M. and Lee, D. 2017. Urn model for products' shares in international trade. – J. Stat. Mech. Theory Exp. 12: 123403.

Barbier, M. and Loreau, M. 2019. Pyramids and cascades: a synthesis of food chain functioning and stability. – Ecol. Lett. 22: 405–419.
Barenblatt, G. I. 1996. Scaling, self-similarity and intermediate asymptotics: dimensional analysis and intermediate asymptotics, Vol. 14. – Cambridge Univ. Press.
Barraquand, F. 2014. Functional responses and predator–prey models: a critique of ratio dependence. – Theor. Ecol. 7: 3–20.
Barraquand, F. and Murrell, D. J. 2013. Scaling up predator–prey dynamics using spatial moment equations. – Methods Ecol. Evol. 4: 276–289.
Beddington, J. R. 1975. Mutual interference between parasites or predators and its effect on searching efficiency. – J. Anim. Ecol. 44: 331–340.
Bettencourt, L. M. et al. 2007. Growth, innovation, scaling and the pace of life in cities. – Proc. Natl Acad. Sci. USA 104: 7301–7306.
Borgmann, U. 1987. Models on the slope of, and biomass flow up, the biomass size spectrum. – Can. J. Fish. Aquatic Sci. 44: s136–s140.
Brose, U. et al. 2019. Predator traits determine food-web architecture across ecosystems. – Nat. Ecol. Evol. 2: 919–927.
Christensen, V. and Walters, C. J. 2004. Ecopath with Ecosim: methods, capabilities and limitations. – Ecol. Model. 172: 109–139.
Cobb, C. W. and Douglas, P. H. 1928. A theory of production. – Am. Econ. Rev. 18: 139–165.
Damuth, J. 1987. Interspecific allometry of population density in mammals and other animals: the independence of body mass and population energy-use. – Biol. J. Linn. Soc. 31: 193–246.
DeAngelis, D. L. et al. 1975. A model for tropic interaction. – Ecology 56: 881–892.
DeLong, J. P. and Vasseur, D. A. 2012. A dynamic explanation of size–density scaling in carnivores. – Ecology 93: 470–476.
DeLong, J. P. et al. 2015. The body size dependence of trophic cascades. – Am. Nat. 185: 354–366.
De Magalhaes, J. and Costa, J. 2009. A database of vertebrate longevity records and their relation to other life-history traits. – J. Evol. Biol. 22: 1770–1774.
Felipe, J. and Fisher, F. M. 2003. Aggregation in production functions: what applied economists should know. – Metroeconomica 54: 208–262.
Geritz, S. and Gyllenberg, M. 2012. A mechanistic derivation of the DeAngelis–Beddington functional response. – J. Theor. Biol. 314: 106–108.
Glazier, D. S. 2015. Is metabolic rate a universal 'pacemaker' for biological processes? – Biol. Rev. 90: 377–407.
Goodnight, C. et al. 2008. Evolution in spatial predator–prey models and the prudent predator: the inadequacy of steady-state organism fitness and the concept of individual and group selection. – Complexity 13: 23–44.
Haond, M. et al. 2018. When higher carrying capacities lead to faster propagation. – bioRxiv: 307322.
Hatton, I. A. et al. 2015. The predator–prey power law: biomass scaling across terrestrial and aquatic biomes. – Science 349: aac6284.
Hatton, I. A. et al. 2019. Linking scaling laws across eukaryotes. – Proc. Natl Acad. Sci. USA 116: 21616–21622.
Hayward, M. W. et al. 2007. The reintroduction of large carnivores to the Eastern Cape, South Africa: an assessment. – Oryx 41: 205–214.
Holling, C. S. 1965. The functional response of predators to prey density and its role in mimicry and population regulation. – Mem. Entomol. Soc. Can. 97: 5–60.
Holt, R. D. and Bonsall, M. B. 2017. Apparent competition. – Annu. Rev. Ecol. Evol. Syst. 48: 447–471.
Keitt, T. H. and Johnson, A. R. 1995. Spatial heterogeneity and anomalous kinetics: emergent patterns in diffusion-limited predatory–prey interaction. – J. Theor. Biol. 172: 127–139.
Kramer, A. M. et al. 2009. The evidence for Allee effects. – Popul. Ecol. 51: 341–354.
Law, R. and Dieckmann, U. 1999. Moment approximations of individual-based models. – Tech. rep. IIASA.
Legendre, P. and Legendre, L. 2012. Dimensional analysis in ecology. – In: Developments in environmental modelling, Vol. 24. Elsevier, pp. 109–142.
Lindeman, R. L. 1942. The trophic-dynamic aspect of ecology. – Ecology 23: 399–417.
Loreau, M. 2010. From populations to ecosystems: theoretical foundations for a new ecological synthesis (MPB-46). – Princeton Univ. Press.
Makarieva, A. M. et al. 2008. Mean mass-specific metabolic rates are strikingly similar across life's major domains: evidence for life's metabolic optimum. – Proc. Natl Acad. Sci. USA 105: 16994–16999.
Morozov, A. and Petrovskii, S. 2013. Feeding on multiple sources: towards a universal parameterization of the functional response of a generalist predator allowing for switching. – PLoS One 8: e74586.
Pascual, M. and Levin, S. A. 1999. From individuals to population densities: searching for the intermediate scale of nontrivial determinism. – Ecology 80: 2225–2236.
Pauly, D. et al. 2000. Ecopath, Ecosim and Ecospace as tools for evaluating ecosystem impact of fisheries. – ICES J. Mar. Sci. 57: 697–706.
Pawar, S. et al. 2012. Dimensionality of consumer search space drives trophic interaction strengths. – Nature 486: 485.
Pels, B. et al. 2002. Evolutionary dynamics of prey exploitation in a metapopulation of predators. – Am. Nat. 159: 172–189.
Pepper, J. W. and Smuts, B. B. 2001. Agent-based modeling of multilevel selection: the evolution of feeding restraint as a case study. – Nat. Resour. Environ. Iss. 8: 10.
Poggiale, J. C. et al. 1998. Emergence of donor control in patchy predator–prey systems. – Bull. Math. Biol. 60: 1149–1166.
Portalier, S. M. et al. 2019. The mechanics of predator–prey interactions: first principles of physics predict predator–prey size ratios. – Funct. Ecol. 33: 323–334.
Ray-Mukherjee, J. et al. 2014. Using commonality analysis in multiple regressions: a tool to decompose regression effects in the face of multicollinearity. – Methods Ecol. Evol. 5: 320–328.
Ripple, W. J. and Beschta, R. L. 2012. Large predators limit herbivore densities in northern forest ecosystems. – Eur. J. Wildl. Res. 58: 733–742.
Schröder, A. et al. 2014. When less is more: positive population-level effects of mortality. – Trends Ecol. Evol. 29: 614–624.
Sjödin, H. et al. 2015. Space race functional responses. – Proc. R. Soc. B 282: 20142121.
Skalski, G. T. and Gilliam, J. F. 2001. Functional responses with predator interference: viable alternatives to the Holling type II model. – Ecology 82: 3083–3092.
Stephens, P. A. et al. 2019. The limits to population density in birds and mammals. – Ecol. Lett. 22: 654–663.

Turchin, P. 2003. Complex population dynamics: a theoretical/empirical synthesis, Vol. 35. – Princeton Univ. Press.
White, C. R. and Seymour, R. S. 2003. Mammalian basal metabolic rate is proportional to body mass2/3. – Proc. Natl Acad. Sci. USA 100: 4046–4049.
Wilson, D. S. 1983. The group selection controversy: history and current status. – Annu. Rev. Ecol. Syst. 14: 159–187.
Wright, S. 1945. Tempo and mode in evolution: a critical review. – Ecology 26: 415–419.
Wynne-Edwards, V. C. 1962. Animal dispersion in relation to social behaviour. – Hafner Pub. Co.
Van Baalen, M. and Sabelis, M. W. 1995. The milker–killer dilemma in spatially structured predator–prey interactions. – Oikos 74: 391–400.
Vucic-Pestic, O. et al. 2010. Allometric functional response model: body masses constrain interaction strengths. – J. Anim. Ecol. 79: 249–256.
Yodzis, P. and Innes, S. 1992. Body size and consumer–resource dynamics. – Am. Nat. 139: 1151–1175.